THE ASTROPHYSICAL JOURNAL, 455:516–523, 1995 December 20

THE GALAXY COMPONENT AND NUCLEAR FLUX MEASUREMENTS OF NGC 5548 FROM DIRECT IMAGING

W. ROMANISHIN,[1,2] T. J. BALONEK,[3] R. CIARDULLO,[1,4] H. R. MILLER,[1,5] B. M. PETERSON,[6] A. C. SADUN,[7] G. M. STIRPE,[8] K. TAKAGISHI,[9] B. W. TAYLOR,[2] AND V. ZITELLI[8]

Received 1993 December 27; accepted 1995 June 26

ABSTRACT

We present the results of analysis of direct imaging data of the galaxy NGC 5548. This galaxy hosts a time-variable active nucleus which has been the focus of intensive spectroscopic monitoring. We focus here on data obtainable from direct imaging of the object. First, we use an image modeling program to derive an image of the galaxy component alone, with the AGN removed, and use such images to study the structure and color of the galaxy. The host galaxy appears to be a relatively normal bulge-dominated (Sa type) spiral, with no evidence of current star formation in the bulge. The derived "AGN-free" images are useful for deriving corrections for the galaxian light that is an inevitable contaminant in spectroscopic and photometric measurements of this object. We discuss how to measure the flux from the nucleus from direct images, and in particular describe a method to obtain photometrically calibrated nuclear flux measurements from less than optimum images. We present nuclear flux values from images contributed by the coauthors, and present flux measurements, corrected for host galaxy light, derived from published photoelectric aperture photometry. We discuss the contamination of the standard spectroscopic aperture by galaxy light. The galaxy flux contamination in the standard spectroscopic aperture derived from the AGN-free images agrees extremely well with that derived from a totally independent spectroscopic method.

Subject headings: galaxies: active — galaxies: individual (NGC 5548) — galaxies: nuclei — galaxies: photometry

1. INTRODUCTION

NGC 5548 is a nearby galaxy ($z = 0.017$) harboring a time-variable active nucleus. This object has been the focus of intensive study of the time variability of the emission lines and continuum from the AGN, using both ground-based (Peterson et al. 1991; Dietrich et al. 1993), *IUE* (Clavel et al. 1991), and *HST* spectroscopy (Korista et al. 1995). Comparison of the time variability in the ionizing continuum from the AGN and the response of the emission lines in the broad-line region (BLR) enables structural information to be obtained about the angularly unresolved BLR. Because NGC 5548 is a fairly bright object and undergoes frequent changes in continuum luminosity, it will undoubtedly continue to be intensively observed in the years ahead.

This contribution focuses on the analysis of direct CCD imaging data on NGC 5548. The optical luminosity of the AGN varies between roughly a tenth and a third that of the host galaxy. One important goal of this study is to produce a best estimate of what the galaxy would look like if it had no AGN. Such an image can be used to remove the inevitable and often times very significant galaxian light component in spectroscopic and photometric measurements. We describe a technique to derive accurate broadband fluxes for the AGN using less than optimum images.

2. OBSERVATIONS

As discussed in Peterson et al. (1991), a large cooperative effort involving many observatories was launched to provide ground-based observations of NGC 5548. Although the emphasis was on spectroscopic data, an appeal was also made by the organizers of the international campaign for direct CCD images of NGC 5548, both to study the galaxy component and to provide measurements of the AGN flux. Although the response to appeals for imaging data has been far less than for spectroscopic data, enough images have been collected to yield useful data on the galaxy component and to provide some additional nuclear flux values.

Thus, there are two separate goals for the analysis of the imaging data: (1) detailed study of the galaxy component of the NGC 5548 system and (2) measurement of accurate flux values from a number of images taken at various times, to provide a check on continuum points derived from the spectroscopic analysis. Ideally, images used for studying the galaxy component in detail must meet a number of criteria: have good seeing, have all pixels in the galaxy image on the linear part of the CCD response, contain not only the AGN but also a sufficiently bright star to determine the point spread function (PSF), be properly flattened (particularly needed to study the outer regions of the galaxy), be photometrically calibrated, and have uniform photometric response (no vignetting). Many of the images contributed had problems meeting one or more of these criteria. In particular, images from smaller telescopes at

[1] Visiting Astronomer, Kitt Peak National Observatory, a division of National Optical Astronomy Observatories, which is operated by the AURA, Inc., under contract with the National Science Foundation.
[2] Department of Physics and Astronomy, University of Oklahoma, Norman, OK 73019.
[3] Department of Physics and Astronomy, Colgate University, Hamilton, NY 13346.
[4] Astronomy Department, Pennsylvania State University, 525 Davey Laboratory, University Park, PA 16802.
[5] Department of Physics, Georgia State University, Atlanta, GA 30303.
[6] Department of Astronomy, Ohio State University, 174 West 18th Avenue, Columbus, OH 43210.
[7] Bradley Observatory, Agnes Scott College, Decatur, GA 30030.
[8] Osservatorio Astronomico di Bologna, Via Zamboni 33, I-40126, Bologna, Italy.
[9] Faculty of Engineering, Miyazaki University, Gakuen-Kibanabdai, Nishi 1.1, Miyazaki, 889-21, Japan.

inferior sites often had very poor seeing and were frequently not flattened very well. However, as discussed below, such images are very useful for obtaining nuclear intensity values, even though they are not useful for studying the host galaxy in detail.

One of the difficulties in studying the host galaxy using image modeling techniques is that NGC 5548 is seen through a rather sparse star field—the nearest star of comparable optical brightness to the nucleus is star 1 of Penston, Penston, & Sandage (1971, hereafter PPS), located ~2.7 from the nucleus of the galaxy. Precise modeling of the nuclear regions requires a PSF star located in the same CCD frame as the galaxy itself because of changes of the PSF over short time intervals. For precise image modeling work, it is highly inadvisable to use PSF stars from separate frames, even those taken immediately before and after the object frames, because the details of the PSF can change significantly from one frame to the next of the same object.

The standard V passband was chosen as the most important imaging filter, because of both its ready availability at all telescopes and the fact that many of the optical spectra covered this region of the spectrum and could be used to understand in detail the spectral composition (lines vs. continuum) of the radiation seen by the imaging detectors. However, as discussed below, not all of the observations use a passband that matches the standard V passband, and color terms were needed to put the images onto a common system. In addition to V, useful images were collected in B, R, and I bandpasses. These have been used to study the color of the host galaxy.

The best V images, in terms of seeing, linear response, and photometric calibration, were obtained by Romanishin on the night of 1989 April 30, using the KPNO 2.1 m telescope and TI CCD. Image FWHM were 0.85, rather better than the typical seeing at Kitt Peak. Unfortunately, the field of view did not permit the inclusion of a PSF star in the same field as NGC 5548 itself, so these images were of limited utility for the image modeling analysis. An excellent V photometric calibration was obtained this night by observation of a number of standard stars from Landolt (1983).

A very useful set of V, R, and I images were obtained by Ciardullo on the night of 1990 April 10 with the TEK 1 CCD on the Kitt Peak 0.9 m telescope. These images contained both NGC 5548 and star 1, although the seeing was not great (~1.6 FWHM). However, these images were taken during an epoch of rather low nuclear luminosity, which aided the determination of the galaxy luminosity profile near the nucleus.

Several useful B images were obtained by Miller in 1989 March, using an RCA CCD on the Kitt Peak 0.9 m telescope. The seeing was 1.7 FWHM.

Little R and I photometry is available for NGC 5548. New photoelectric photometry was obtained by Romanishin and BWT on the night of 1991 June 15, using the 0.76 m Lowell/NURO telescope on Anderson Mesa. Results of this photometry are as follows: in a 29.2 diameter aperture, $V = 13.18$, $V-R = 0.51$, $R-I = 0.38$; in a 83.2 diameter aperture, $V = 12.70$, $V-R = 0.51$, $R-I = 0.47$. These measurements used standard stars from Landolt (1983).

Of the available CCD images, only the Romanishin V images were obtained under known photometric conditions and had sufficient observations of standard stars to enable a good photometric calibration. To provide an independent check on this V photometric calibration, and to provide calibration in the other colors, we turned to published photoelectric photometry. Because of the variability of the nucleus, we used magnitudes in annuli formed by differencing magnitudes found in two concentric apertures to set the zero point of the CCD images. We caution, however, that this procedure is fraught with potential errors: the photoelectric photometry observations may have been not precisely centered on the galaxy nucleus, the seeing may have been poor, the apertures sizes may not have been precisely measured, and the annular magnitude, being a difference of two (noisy) measurements has a higher uncertainty than either aperture measurement alone.

We used a number of independent photoelectric measurements. We used published photoelectric photometry meeting the following criteria: measurements in at least two apertures, with the smaller aperture at least 15″ in diameter (to obviate seeing and centering problems) and the larger aperture at least twice the diameter of the smaller (to ensure a good signal), measurements taken on the same night (to ensure the nucleus had same intensity). If more than one pair of apertures was available, each nights data were averaged. Ten sets of aperture photometry were found: two from Burstein et al. (1987), five from de Vaucouleurs, de Vaucouleurs, & Corwin (1978), one from McAlary et al. (1983), one from Weedman (1973), and one from the Lowell/NURO photometry described previously. In addition to these photoelectric annular magnitudes, an independent calibration was obtained from the CCD-derived annular magnitudes of MacKenty (1990), the Romanishin V CCD data, and from star 1 of PPS, for a total of 13 independent photometric measurements of extranuclear regions of NGC 5548 in V.

The Ciardullo image was considered as the "standard" V image. For each annulus, we performed synthetic aperture photometry of this image using the PHOT command in the APPHOT package in IRAF. Comparison of the CCD instrumental magnitude and the annular magnitudes yielded 13 values of the photometric zero point for the standard image. The rms scatter in the zero points was 0.06 mag, yielding a formal mean error of 0.016 mag. This final zero point matches that of the Romanishin V CCD data to within 0.01 mag. Given that the average photoelectric measurement has an error of something like 0.03–0.04 mag in each aperture, the final scatter in independently derived zero points is quite good.

In B, there were 11 measurements (no 2.1 m or Lowell/NURO photometry), yielding a zero-point rms scatter of 0.06 mag and a formal error in the mean of 0.02 mag. In (Kron-Cousins) R, only three measurements are available: from Lowell/NURO photometry, McAlary et al. (1983), and MacKenty (1990). These again yield a formal scatter of 0.06 mag for a formal error in the mean of 0.04 mag. In (Kron-Cousins) I, only two suitable measurements are available: from Lowell/NURO photometry, and McAlary et al. (1983). These two zero points differ by 0.12 mag.

Once the final zero points of the "standard" images were determined, these images were used to determine the magnitudes of star 1 of PPS. This is an important star because it has been used to provide a zero point for photometric measurements of NGC 5548. The following values were found, integrating all the light in a 20″ diameter aperture: $V = 13.75$, $B-V = 0.71$, $V-R = 0.39$, and $R-I = 0.31$. This V magnitude differs from that of PPS by 0.05 mag, while the B mag differs by only 0.01. Because the magnitudes derived here use a number of independent measurements to derive the zero point, while PPS observed star 1 only once, we consider the magnitudes and colors reported here to be superior to those of PPS.

3. ANALYSIS

3.1. *AGN and Host Galaxy Separation*

The luminosity of the host galaxy and the unresolved AGN source, and uncertainty in the AGN flux, were estimated using the image modeling program developed by WR. Details of the program are given in Romanishin & Hintzen (1989) and in Smith et al. (1986). For each of the four final images, we carefully made the best fit to the luminosity profile, assuming the observed profile is the result of a galaxy plus unresolved point source component, convolved with the PSF which is primarily determined by the seeing. Basically, we made models of the galaxy consisting of a pure exponential disk component and a $r^{1/4}$ bulge. Different "types" of spirals are assumed to have different bulge to disk luminosity ratios (B/D) and different ratios of the bulge effective radius (r_e) and disk scale length (α^{-1}) size scales. For each galaxy type, average values of B/D and the size scale ratio were taken from the work of Boroson (1981). We then made a large number of model galaxy plus point source images, varying the B/D ratio and the overall size scale of the galaxy, convolved these with the point spread function, and compared the surface brightness profile of the smeared model with that observed. For NGC 5548, only model host galaxies with a large bulge component (Sa type with B/D = 1.2) gave an acceptable fit to the luminosity profile. The surface brightness profiles are shown in Figures 1 and 2. Figure 1 shows the full fitting range, from 0″ to 35″ radius. The profile of the smeared best fit model (Sa + point source) is shown. This fits the overall shape of the observed profile well, particularly in the range of 0″–7″. (From 15″ to 35″ the galaxy shows deviations from a pure exponential disk, as do most galaxies, but the overall shape is well fitted by the model.) Also shown is the "best-fit" Sb model. This fit is clearly inferior. In particular, it cannot fit the profile in the 3″–7″ range, as it does not have enough "bulge" light. We must note that real galaxies of a given (visually assigned) type can vary widely in B/D values (Boroson 1981), so that the "type" assigned from the profile fitting may be different from the visually assigned type. After determining the best-fit point source, the PSF was appropriately scaled in flux and subtracted from the observed image, leaving the image of the host galaxy alone.

This "AGN-free" galaxy image can be used to estimate the galaxian V light contribution through various size apertures and slit sizes, to allow a derivation of the luminosity of the nucleus from observation which naturally include both nucleus and galaxy light. These nucleus free images have seeing of $\sim$1.″7 FWHM. We modeled the effects of poorer seeing (frequently encountered on some of the images taken from little telescopes at inferior sites) by convolving these images with appropriate Gaussians to simulate inferior seeing.

Using the AGN-free galaxy images, we derived the color profiles of the host galaxy. The V, R, and I images were obtained with the same telescope and detector, so we derived the $V-I$ profile (Fig. 3) by simply ratioing the galaxy fluxes, averaged around circular annulli of width 1 pixel, and converting to a color. The B image was obtained with a different detector, and so we could not easily obtain the color profile as for $V-I$. Instead, we obtained the magnitudes (and hence colors) in annuli 2″ in width by differencing aperture measurements made with PHOT (discussed in more detail below). The error bars shown for both color profiles were derived by subtracting different amounts of AGN contribution, corresponding to the AGN flux uncertainty limits. As expected, the central few pixels are greatly affected by the uncertainty limits luminosity, but at radii larger than a few arcseconds the color is hardly affected by the AGN. The color profile of the galaxy shows the general form expected for a early-type spiral galaxy with a very prominent bulge component: the central regions are red, and the outer regions bluer. The best-fit galaxy model has a bulge effective radius of $\sim$7″, which matches well with the region showing the red color. The central colors,

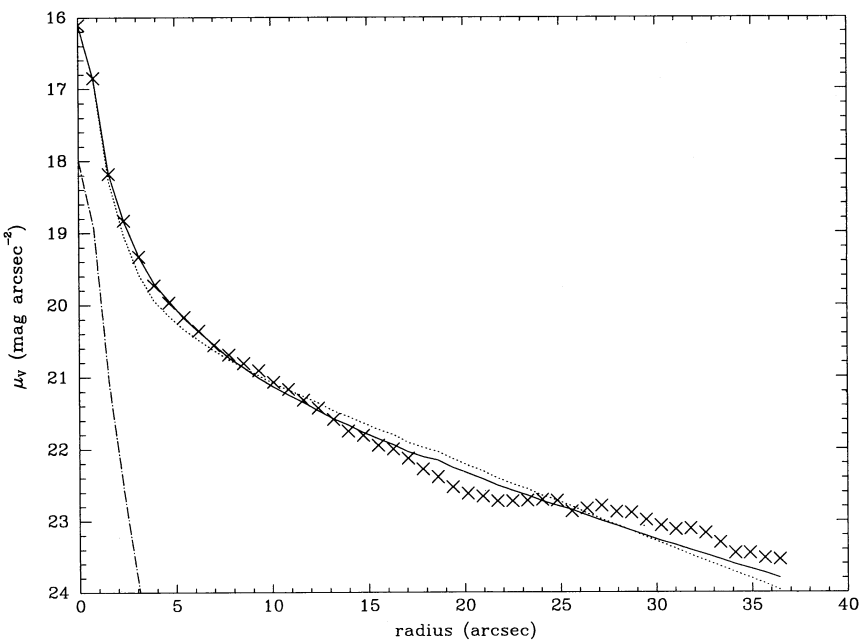

FIG. 1.—The observed and modeled V surface brightness profile of the central region of NGC 5548. The crosses denote the observed surface brightness profile of the V image. The solid line is the best-fit point source + "Sa" model galaxy, convolved with the PSF. The dotted line is the best fit point source + "Sb" model galaxy, convolved with the PSF. The dot-dash line shows the point source, convolved with the point source function.

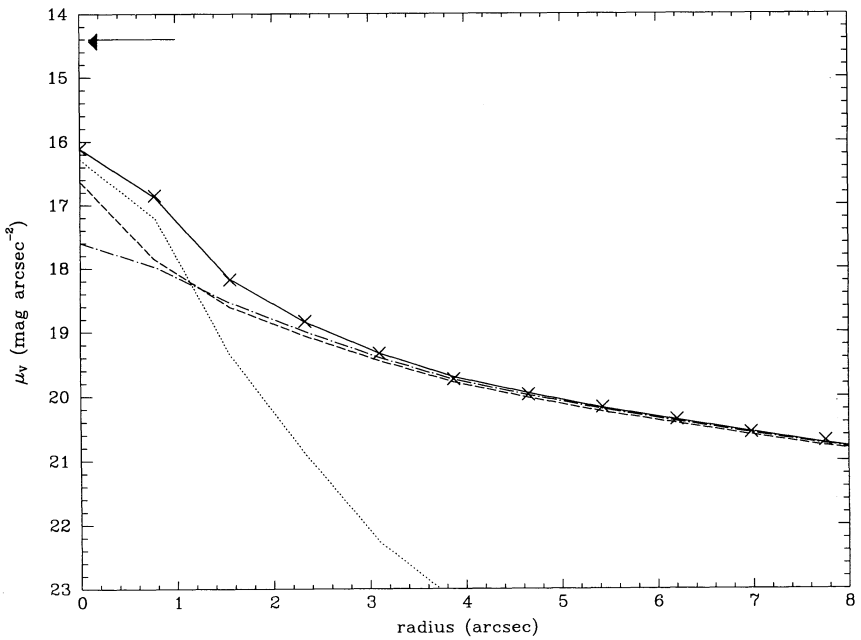

FIG. 2.—This shows the central 8″ radius of the V-band profile of NGC 5548. The crosses denote observed points. The solid line is the best-fit smeared point source plus galaxy model. The dashed line is the best model galaxy with no atmospheric smearing, and the smeared galaxy profile (this is our best guess as to what the galaxy would look like with no central point source) is shown by the dash-dot line. The dotted line shows the point source, convolved with the point source function. The magnitude of the central point source is shown by the arrow.

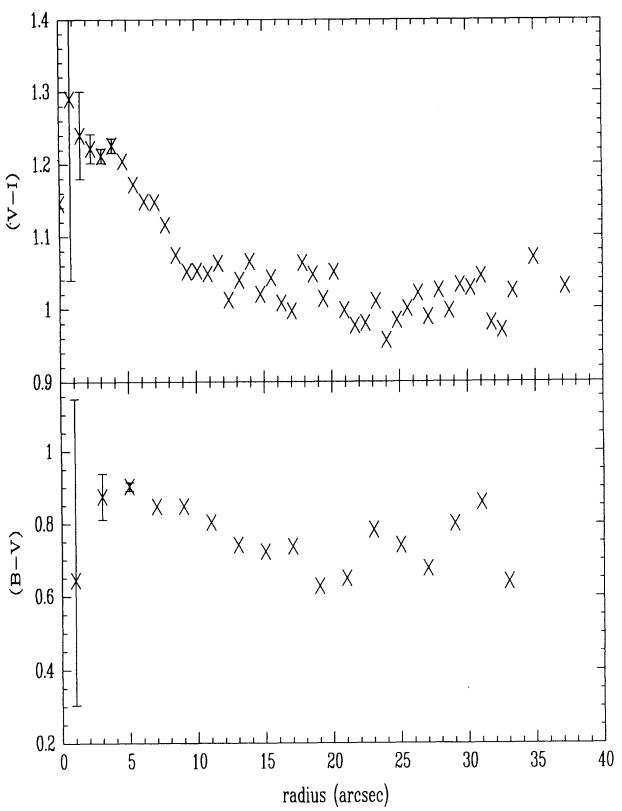

FIG. 3.—The color profiles of AGN-free NGC 5548 galaxy. The error bars at small radii show the effects of uncertainty in the nuclear flux derived from the image modeling program. The top panel shows the $V-I$ profile, the bottom the $B-V$ profile.

$V-I \sim 1.2$, $B-V \sim 0.9$, are similar to the colors of an elliptical galaxy (unpublished photoelectric photometry in the Cousins system by WR gives $V-I = 1.22$, $B-V = 0.96$ for the central regions of a half-dozen E galaxies). The colors in the "disk dominated" region, beyond $\sim 20''$ ($B-V \sim 0.75$ and $V-I \sim 1.0$) match colors for disk-dominated galaxies. Thus, within the uncertainties of the central region colors, dominated by the AGN subtraction, the galaxy has a color profile expected from a bulge-dominated disk galaxy. Thus, this analysis shows no evidence for a wide-spread nuclear starburst, sometimes seen in quasars (Romanishin & Hintzen 1989). Obviously, a physically small region of intense star formation activity could be present but not be separable from the nonthermal nuclear component.

Aperture magnitudes of the AGN-free galaxy in each of the four colors are given in Table 1. For each color, three sets of magnitudes are given, corresponding to subtraction of the best estimate of the AGN, and also subtraction of an AGN fainter (or brighter) by the estimated error of the point source flux determination. These magnitudes were derived using the IRAF task PHOT in the DIGIPHOT/APPHOT package. The magnitudes are quoted to thousandths of a magnitude only to enable accurate differences to be taken. These magnitudes are taken from the point-spread subtracted observed image, and so are our best guess of what the galaxy would look like with the seeing conditions present ($\sim 1''.7$ for all images).

3.2. *AGN Flux*

The second goal of the analysis of the imaging data is to obtain measurements of the broadband flux from the AGN component in NGC 5548. Although the best method to do this would be to do a full modeling analysis on each image, this is not possible for frames which do not have a PSF star. Our

TABLE 1

APERTURE MAGNITUDES OF AGN-FREE GALAXY IMAGES

	B			V			R			I		
Radius (arcsec)	best AGN	faint AGN	bright AGN	best AGN	faint AGN	bright AGN	best AGN	faint AGN	bright AGN	best AGN	faint AGN	bright AGN
1.00	17.398	16.946	18.187	16.920	16.758	17.112	16.364	16.233	16.513	15.655	15.484	15.857
2.00	16.361	16.022	16.857	15.717	15.628	15.814	15.117	15.050	15.187	14.462	14.364	14.569
3.00	15.865	15.610	16.197	15.142	15.085	15.201	14.533	14.491	14.576	13.902	13.838	13.969
4.00	15.569	15.365	15.821	14.799	14.757	14.843	14.183	14.152	14.215	13.565	13.517	13.615
5.00	15.353	15.180	15.558	14.556	14.521	14.591	13.936	13.911	13.962	13.326	13.287	13.366
6.00	15.178	15.029	15.352	14.366	14.337	14.395	13.749	13.728	13.771	13.145	13.111	13.180
7.00	15.033	14.900	15.185	14.214	14.189	14.240	13.598	13.580	13.617	13.003	12.973	13.033
8.00	14.908	14.788	15.043	14.088	14.066	14.111	13.475	13.459	13.492	12.885	12.858	12.912
9.00	14.795	14.686	14.917	13.975	13.955	13.996	13.369	13.354	13.384	12.783	12.759	12.808
10.00	14.700	14.599	14.812	13.875	13.856	13.894	13.276	13.262	13.290	12.694	12.672	12.717
11.00	14.611	14.517	14.714	13.788	13.770	13.805	13.195	13.182	13.208	12.616	12.595	12.637
12.00	14.533	14.445	14.628	13.711	13.695	13.727	13.123	13.111	13.135	12.548	12.528	12.568
13.00	14.465	14.382	14.554	13.644	13.629	13.660	13.058	13.047	13.070	12.489	12.470	12.508
14.00	14.401	14.323	14.486	13.588	13.573	13.602	13.002	12.991	13.012	12.438	12.420	12.456
15.00	14.345	14.270	14.425	13.537	13.523	13.551	12.954	12.944	12.965	12.392	12.375	12.409
16.00	14.296	14.224	14.372	13.491	13.478	13.504	12.911	12.901	12.921	12.350	12.333	12.367
17.00	14.251	14.182	14.324	13.448	13.435	13.461	12.871	12.862	12.881	12.312	12.296	12.328
18.00	14.211	14.145	14.281	13.411	13.399	13.423	12.838	12.828	12.847	12.278	12.263	12.294
19.00	14.173	14.109	14.241	13.379	13.367	13.391	12.809	12.800	12.818	12.249	12.234	12.264
20.00	14.141	14.079	14.207	13.351	13.339	13.363	12.782	12.773	12.790	12.224	12.209	12.238
21.00	14.110	14.050	14.174	13.324	13.313	13.336	12.756	12.747	12.764	12.199	12.185	12.214
22.00	14.082	14.024	14.145	13.299	13.288	13.310	12.732	12.723	12.740	12.176	12.162	12.191
23.00	14.056	13.998	14.116	13.273	13.262	13.284	12.708	12.700	12.717	12.154	12.140	12.167
24.00	14.029	13.973	14.088	13.246	13.236	13.257	12.685	12.677	12.693	12.130	12.116	12.144
25.00	14.003	13.948	14.060	13.220	13.210	13.230	12.659	12.652	12.667	12.106	12.093	12.119
26.00	13.976	13.923	14.032	13.195	13.185	13.205	12.636	12.628	12.644	12.082	12.069	12.095
27.00	13.947	13.895	14.002	13.170	13.160	13.180	12.612	12.604	12.619	12.058	12.046	12.071
28.00	13.920	13.869	13.974	13.144	13.135	13.154	12.586	12.578	12.593	12.035	12.023	12.048
29.00	13.896	13.847	13.949	13.120	13.111	13.129	12.562	12.555	12.569	12.013	12.001	12.025
30.00	13.874	13.825	13.925	13.097	13.088	13.107	12.541	12.534	12.548	11.992	11.980	12.004
31.00	13.855	13.807	13.905	13.076	13.067	13.085	12.522	12.515	12.529	11.972	11.961	11.984
32.00	13.835	13.788	13.884	13.055	13.047	13.064	12.503	12.497	12.510	11.953	11.942	11.965
33.00	13.814	13.768	13.862	13.035	13.027	13.044	12.487	12.480	12.493	11.936	11.924	11.947
34.00	13.793	13.747	13.840	13.018	13.009	13.027	12.471	12.465	12.478	11.919	11.908	11.930
34.44	13.784	13.739	13.831	13.011	13.003	13.020	12.465	12.459	12.472	11.912	11.901	11.923
35.00	13.775	13.730	13.821	13.002	12.994	13.011	12.458	12.451	12.464	11.903	11.893	11.915
40.00	13.693	13.651	13.736	12.941	12.934	12.950	12.402	12.396	12.408	11.844	11.833	11.854
45.00	13.647	13.607	13.688	12.902	12.894	12.909	12.364	12.358	12.370	11.798	11.788	11.808
50.00	13.606	13.568	13.646	12.872	12.864	12.879	12.340	12.334	12.346	11.771	11.761	11.781
55.00	13.565	13.528	13.603	12.853	12.846	12.861	12.326	12.320	12.332	11.752	11.742	11.761
60.00	13.531	13.495	13.568	12.838	12.830	12.845	12.323	12.317	12.329	11.737	11.728	11.747
65.00	13.501	13.466	13.537	12.823	12.816	12.831	12.318	12.312	12.323	11.722	11.713	11.731
70.00	13.472	13.438	13.507	12.807	12.800	12.814	12.310	12.304	12.315	11.706	11.697	11.715
75.00	13.436	13.404	13.470	12.789	12.782	12.796	12.297	12.292	12.303	11.689	11.680	11.698

approach to measuring the AGN flux from CCD images uses synthetic aperture photometry, with corrections for the effects of poor seeing and for the inevitable galaxian contamination from the AGN-free images.

Of the images contributed, none were obtained under strictly photometric conditions, with adequate observations of photometric standard stars to accurately define the photometric zero point and color transformations. Thus, we are forced to use only the information in each image itself to derive the photometric calibration zero point. Some images contained both the galaxy and star 1, and so this star could be used for the zero point. However, since this star is 2.7 from the galaxy, problems such as vignetting and poor flat fielding could compromise the zero point. For images for which star 1 could not be used to find the calibration, we have developed a technique, described below, to use the galaxy component itself to provide the photometric zero point.

Any attempt to measure the AGN flux by photometry of images must correct for the contamination by the galaxy signal. The galaxy and AGN signal in any aperture depends on the seeing. Thus, although we might want to use a very small aperture to maximize the AGN/galaxy ratio, the galaxy contribution as well as AGN signal are particularly uncertain in small apertures due to small seeing changes. We therefore use an 8″ radius aperture as a compromise between minimizing galaxy contribution and making sure we get all the AGN flux. To estimate the galaxy contribution to the signal in the 8″ aperture for any image, we use the following technique; We measure the signal in apertures of radius 8″, 25″, and 34.″44. We could, in principle, use the signal in one of the annuli defined

by the three apertures to estimate the galaxy signal in the 8″ aperture, but if the sky value is not determined very accurately (a problem with poorly flattened images), the annular signal can be substantially in error. Instead, we measure the *difference* signal between the 8″–25″ and 25″–34.″4 annuli. These annuli have identical areas, so the sky contribution cancels, which leaves just the signal from the galaxy in the inner annulus minus the (lower) signal from the galaxy in the outer annulus. For a given value of the seeing, there is a fixed ratio of galaxy flux in the 8″ aperture and the difference signal. For images with poor seeing, the ratio is lower, as light from the 8″ aperture spills over into the inner annulus. To find the ratio as a function of seeing, we have taken the standard nucleus-free V image, and convolved it with Gaussians to mimic poorer seeing, and measured the ring difference and 8″ signal ratio for these artificially degraded images.

Thus, to estimate the galaxy contribution to the central aperture, we estimate the seeing FWHM for each image, using a star, or the nucleus itself if no star is in the image, measure the ring difference signal, and multiply that by the ratio of 8″ aperture signal to ring difference signal for the appropriate seeing. We can then subtract the galaxy signal from the measured central signal to get the signal from the nucleus alone. Of course, we must also subtract the sky level from the 8″ aperture, but since the signal level is high, uncertainties in the sky level do not introduce significant errors. For seeing of 2.″5 or better, virtually all the light from the AGN is contained in the 8″ aperture. For poorer seeing, some AGN light spills over into the 8″–25″ ring. If AGN spillover is a problem, the 8″–25″ ring signal is corrected in an iterative way: first the AGN flux is estimated, ignoring spillover, then this flux is used to estimate the spillover signal in the ring, and the ring signal is corrected, and this corrected signal used to estimate the galaxy signal in the central aperture. For example, ~10% of the light from a point source lies outside the central aperture for seeing of 4″ FWHM.

Once we have the signal of the isolated AGN, we must have a zero point to find a true V magnitude. For images which include star 1, the zero point can be derived from that star. The color of star 1, at least from V redward to I, is similar to that of a $\nu^{-0.7}$ power law, so there is no significant color correction needed when using star 1 to set the zero point for the nuclear magnitude.

We can also derive the zero point from the galaxy itself. For the standard V image, the V magnitude of the ring difference signal is 14.39. Poorer seeing causes the ring difference to brighten, as galaxy light from the central aperture spill into the inner ring, so we have measured the ring difference magnitude as a function of seeing from the artificially degraded standard image. Because the ring signal is much redder than the nucleus, color effects can enter. Although the effect is relatively small, we have corrected for it as follows. For each individual filter curve, we have convolved the filter and detector responses with spectra of galaxies, or a power law for the AGN, of colors approximately equal to the true observed colors of the objects. By comparing the "signals" from the convolutions in the standard V passband and for the observed responses, we are able to calculate the zero point offset from the annular zero point for the central regions of the galaxy and for the AGN.

The V seeing correction is shown in Figure 4. The top panel shows the magnitude of the central 8″ region, and the magnitude of the difference signal between the 8″–25″ and 25″–34.″4 annuli, as a function of seeing.

Whenever possible, the zero points were derived from both the ring difference method and from star 1. From limited night-to-night consistency checks, it appears that the use of star 1 to find the zero point is preferable, particularly for images from small telescopes which are read-out noise limited, so that the large number of pixels in the rings contribute to a relatively low S/N ratio. However, particularly for well exposed images, the ring difference can yield good zero points, if care is taken to take account of the effects of seeing.

Table 2 lists the magnitudes of the nucleus (V_{nuc}) derived from the contributed images. The points are too sparse to

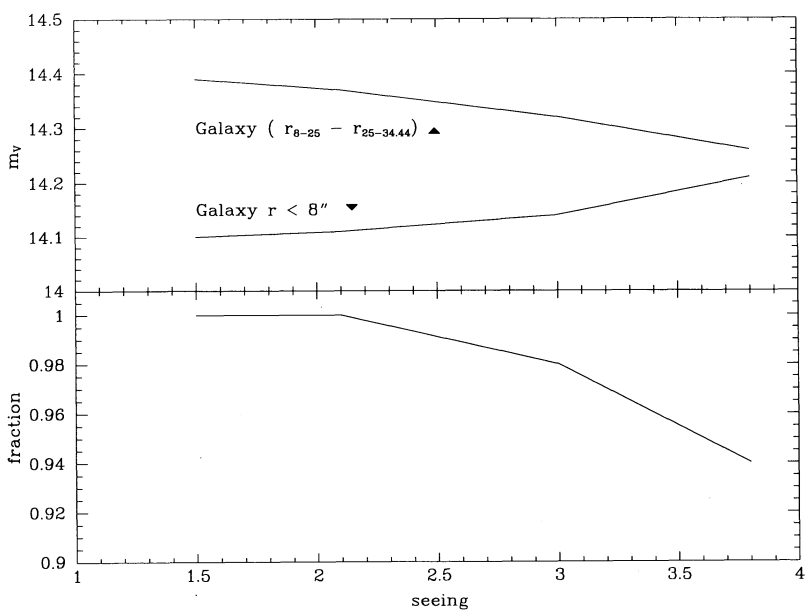

FIG. 4.—The seeing correction. The top panel shows the V magnitude in the inner 8″ radius, and in the annular difference magnitude, as a function of the FWHM seeing. The lower panel shows the fraction of light from a point source that falls in an 8″ radius aperture for various values of the seeing.

TABLE 2

V MAGNITUDES OF NGC 5548 AGN

UT Date	Time	Julian Date (2,440,000+)	V_{nuc}	Observer[a]
1989 Jan 27	18:59	7554.3	14.22	KT
1989 Jan 28	19:33	7555.3	14.32	KT
1989 Mar 15	09:21	7600.9	14.34	HRM
1989 Mar 17	08:09	7602.8	14.32	HRM
1989 Mar 18	08:28	7603.8	14.37	HRM
1989 Mar 20	08:01	7605.9	14.25	AS
1989 Mar 21	08:46	7606.9	14.22	AS
1989 Mar 22	09:42	7607.9	14.08	AS
1989 Mar 23	07:57	7608.8	14.08	AS
1989 Mar 24	08:32	7609.9	14.24	AS
1989 Mar 28	15:18	7614.1	14.14	KT
1989 Mar 29	15:31	7615.1	14.06	KT
1989 Mar 29	22:42	7615.4	14.12	GMS+VZ
1989 Apr 30	09:20	7646.9	14.08	WR
1989 May 7	13:07	7654.0	14.31	KT
1989 May 18	05:47	7664.7	14.24	TJB
1989 May 18	04:51	7664.7	14.24	AS
1989 May 19	10:08	7665.9	14.27	AS
1989 May 20	06:02	7666.8	14.20	AS
1989 May 21	06:47	7667.8	14.30	AS
1989 Dec 20	12:00	7881.0	14.44	AS
1989 Dec 23	13:00	7884.0	14.47	AS
1989 Dec 24	13:00	7885.0	14.44	AS
1990 Apr 10	08:50	7991.9	14.96	RC
1990 May 25	14:08	8037.1	14.85	KT
1990 May 26	15:49	8038.1	14.70	KT
1990 May 28	14:57	8040.1	14.68	KT
1990 Jun 11	12:43	8054.0	14.75	KT
1990 Jun 19	14:05	8062.0	14.80	KT
1990 Jun 20	12:27	8063.0	14.89	KT

[a] Telescopes used: KT: Kagoshima Space Center 0.6 m; HRM: Kitt Peak 0.9 m; AS: Lowell 1.1 m; GMS+VZ: Loiano 1.5 m; WR: Kitt Peak 2.1 m; TJB: Foggy Bottom Obs. 0.4 m; RC: Kitt Peak 0.9 m.

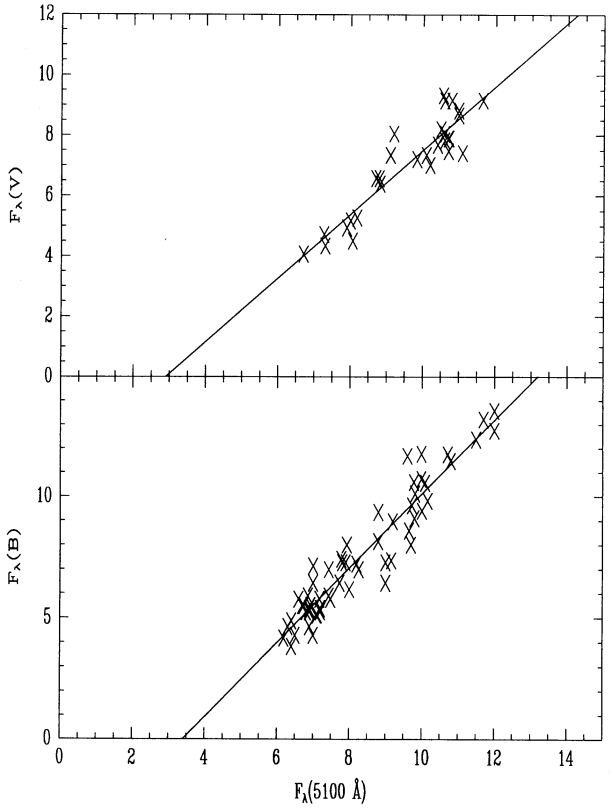

FIG. 5.—The nuclear flux derived from (*top panel*) V images [$F_\lambda(V)$] and nuclear flux from (*bottom panel*) Balonek B images [$F_\lambda(B)$] plotted against F_λ(5100), the spectroscopically derived continuum flux of nucleus and central parts of the galaxy. Fluxes are in units of 10^{-15} ergs s^{-1} cm^{-2} Å^{-1}.

make a good light curve, but it is useful to compare these nuclear flux values to the F_λ(5100) continuum values derived spectroscopically by Peterson et al. (1992). We convert the V_{nuc} magnitudes into fluxes using the conversion of Johnson (1966). The top panel of Figure 5 shows $F_\lambda(V)$ versus F_λ(5100). The quantities show a linear relation, with a nonzero intercept on the F_λ(5100) axis. This is due to the fact that F_λ(5100) is not a pure nuclear flux, but also contains the galaxy flux in the $5'' \times 7''.6$ aperture used in the spectroscopy, as discussed below. Because of the sparse spacing of the V_{nuc} points, and source variability, it is difficult to intercompare the different observers values. Only three pairs of V_{nuc} values from different observers, taken within a span of 3 days or less, are available. The average difference between the three pairs is 0.05 mag. Another measure of the uncertainty in V_{nuc} comes from the scatter of the points around the best fit of $F_\lambda(V)$ versus F_λ(5100), discussed below. The scatter around the best-fit line is 0.09 mag. As this assumes the F_λ(5100) values are errorless, the true observational dispersion in V_{nuc} must be less than this.

3.3. *AGN Flux from Aperture Photometry*

Once we have a "nucleus-free" image, we can use this to correct aperture photometry for galaxy contamination and derive estimates of the AGN flux from single aperture photometric measurements.

Of particular interest is the extensive list of B aperture measurements determined by Balonek from aperture photometry of CCD images, calibrated with star 1 (see Peterson et al. 1991, 1992). To derive B fluxes of the nucleus alone, we subtracted the galaxy signal, derived from the B nucleus-free image in the aperture used by Balonek (17".5 diameter), and converted these magnitudes into fluxes with the conversion from Johnson (1966). The lower panel of Figure 5 shows $F_\lambda(B)$ versus F_λ(5100).

"Historical" (pre–AGN Watch) photoelectric photometry measurements mentioned earlier were used to calculate values of V_{nuc}, using the standard V image to derive galaxy contributions in each aperture. Although there are only about a dozen epochs, scattered over 25 years, this data is worth a look to see if there has been any radical change in AGN flux over the last few decades. A few published photometry points are not included because the dates of observations were not published. The derived values of V_{nuc} are listed in Table 3. The errors are estimated by intercomparing values from different sized apertures, when available, otherwise they are estimated by assuming that the photometry magnitudes have uncertainties of 0.03 mag. The majority of the V_{nuc} values range between 14 and 15, the range covered during the spectroscopic campaign. Of note in these historical data is a point from 1982 July ($V_{nuc} = 13.83$), marginally brighter than any measured during the campaign, two points about a factor of 2 fainter than the faintest level recorded during the campaign ($V_{nuc} = 15.55$ in February 1976 and $V_{nuc} = 15.75$ in 1979 March), and a change in AGN flux of a factor of almost factor of 3 within 20 days in 1973 March–April.

TABLE 3

V MAGNITUDES OF NGC 5548 AGN FROM HISTORICAL PHOTOELECTRIC PHOTOMETRY

UT Date	Julian Date (2,440,000+)	V_{nuc}	Estimate Error	Photometry Reference
1968 Mar 25	39941	14.86	0.2	DEV72
1968 Mar 28	39944	14.26	0.1	DDC78
1968 Mar 29	39945	14.13	0.15	DEV72
1968 Apr 4	39951	14.43	0.1	DEV72
1968 Apr 5	39952	14.20	0.1	DDC78
1968 Apr 5	39952	14.12	0.1	DEV72
1971 Apr 26	41068	14.61	0.1	DDC78
1972 Mar 13	41390	14.79	0.1	DDC78
1972 Mar 18	41395	14.83	0.2	DDC78
1973 Mar 13	41755	15.10	0.3	DDC78
1973 Apr 1	41774	13.94	0.06	DDC78
1975 Apr 10	42513	14.65	0.2	DDC78
1976 Feb 26	42385	15.55	0.2	DDC78
1978 Apr 3	43602	13.97	0.06	LER80
1979 Mar 7	43940	15.75	0.3	LER80
1980 Apr 15	44345	14.02	0.06	MMM83
1982 Jul 23	45174	13.83	0.06	DDP84

REFERENCES.—DDP84: Dibai, Doroshenko, & Postnov 1984; DEV72: de Vaucouleurs & de Vaucouleurs 1972; DDC78: de Vaucouleurs, de Vaucouleurs, & Corwin 1978; LER80: Lebofsky & Rieke 1980; MMM83: McAlary et al. 1983.

3.4. *Galaxy Contribution to $F_\lambda(5100)$*

Linear least-squares fits to $F_\lambda(V)$ and $F_\lambda(B)$ versus $F_\lambda(5100)$ give

$$F_\lambda(V) = 1.057 \pm 0.08 \times [F_\lambda(5100) - 2.9 \pm 0.7]$$

and

$$F_\lambda(B) = 1.525 \pm 0.06 \times [F_\lambda(5100) - 3.4 \pm 0.4] ,$$

where all fluxes are measured in units of 10^{-15} ergs s^{-1} cm^{-2} Å^{-1}. These fits are shown in Figure 4. The nonzero intercept gives the value of the galaxy flux in the standard 5″ × 7.″6 aperture used by the spectroscopists.

Once the intercepts were determined, they were subtracted from the $F_\lambda(5100)$ values, and the fits redone, after converting to magnitudes. These fits show, within the errors, a unit slope relation between V_{nuc} and B_{nuc} and the 5100 Å nuclear magnitude. The scatter around these fits, assuming the $F_\lambda(5100)$ values are errorless, are 0.09 mag in V and 0.12 mag in B. The B scatter is quite low, considering that these were taken with a 0.4 m telescope. Much of the relatively low scatter is probably due to the fact that the nucleus to galaxy ratio is higher in B than in V, so subtraction of the galaxy is less crucial. The value of the $F_\lambda(5100)$ contamination flux derived from the B data, which is superior to that determined from the V data because of a larger number of points, is virtually identical to the value ($3.37 \pm 0.54 \times 10^{-15}$ ergs s^{-1} cm^{-2} Å^{-1}) found from comparing *IUE* and 5100 Å fluxes by Peterson (1991).

Another measure of the galaxy contribution to the 5″ × 7.″6 aperture was determined by measuring the V magnitude of the nucleus-free V image, through an aperture of size 5″ × 7.″6 aperture, long axis east-west. This gives $V = 14.99$,

Note that this flux cannot be directly compared with the $F_\lambda(5100)$ value derived above for the galaxy contamination, because of the different wavelength and passband of the two measurements. To compare these numbers we first scaled an off-nucleus spectrum of NGC 5548 to $F_\lambda(5100) = 3.4 \times 10^{-15}$ ergs s^{-1} cm^{-2} Å^{-1}, and then convolved this scaled spectrum with a V filter to determine the corresponding V mag for an object with the off-nuclear spectrum and that flux at 5100 Å. This V magnitude turned out to be 14.99, identical to that derived directly from the nucleus-free image.

4. DISCUSSION AND CONCLUSIONS

We have developed a technique for deriving accurate AGN magnitudes for AGNs with prominent host galaxies from less than ideal CCD observations. This technique obviates the problems of nonphotometric conditions, poor seeing, and poor flattening which sometimes are found in observations taken with smaller telescopes. We hope this technique will be useful for imaging analysis of AGNs with prominent host galaxies, which are becoming more readily observable due to the increasing availability of CCDs on many small telescopes.

Our main conclusions are follows:

1. The galaxy component of NGC 5548 appears consistent with it being a "normal" early-type spiral. The luminosity profile of the object is well fitted by an unresolved point source and a disk + bulge galaxy component. The color profile is also quite consistent with a early-type spiral, with no conclusive evidence of current star formation in the bulge. The nucleus-free images derived will be useful for correcting photometric and spectroscopic measurements for the galaxian light contribution.

2. The galaxian light contribution to the standard spectroscopic 5″ × 7.″6 aperture derived from the AGN-free images is equal, to within the errors, to that derived by comparison of *IUE* and 5100 Å fluxes.

3. Smaller telescopes *can* produce worthwhile data on this and similar objects, even if observing conditions are far from ideal. The most important guideline for observers is to obtain enough photons to minimize uncertainty due to photon noise, but to use exposures short enough to make sure all pixels in the galaxy image, as well as the PSF star, are on the linear part of the CCD response curve.

B. M. P. acknowledges financial support from NSF grant AST-9117086 and STScI grant GO-3484.01.91A. A. C. S. acknowledges telescope time from Lowell Observatory.

REFERENCES

Boroson, T. 1981, ApJS, 46, 177
Burstein, D., Davies, R. L., Dressler, A., Faber, S. M., Stone, R. P. S., Lynden-Bell, D., Terlevich, R. J., & Wegner, G. 1987, ApJS, 64, 601
Clavel, J., et al. 1991, ApJ, 366, 64
Dibai, E. A., Doroshenko, V. T., & Postnov, K. A. 1984, Soviet Astron., 28, 1
de Vaucouleurs, G., & de Vaucouleurs, A. 1972, MmRAS, 77, 1
de Vaucouleurs, G., de Vaucouleurs, A., & Corwin, H. G. 1978, AJ, 83, 1331
Dietrich, M., et al. 1993, ApJ, 408, 416
Johnson, H. L. 1966, ARA&A, 4, 193
Korista, K. T., et al. 1995, ApJS, 97, 285
Landolt, A. U. 1983, AJ, 88, 439
Lebofsky, M. J., & Rieke, G. H. 1980, Nature, 284, 410
MacKenty, J. W. 1990, ApJS, 72, 231
McAlary, C. W., McLaren, R. A., McGonegal, R. J., & Maza, J. 1983, ApJS, 52, 341
Penston, M. J., Penston, M. V., & Sandage, A. 1971, PASP, 83, 783
Peterson, B. M. 1991, in Variability of Active Galaxies, ed. W. J. Duschl, S. J. Wagner, & M. Camenzind (Berlin: Springer), 47
Peterson, B. M., et al. 1991, ApJ, 368, 119
———. 1992, ApJ, 392, 470
Romanishin, W., & Hintzen, P. 1989, ApJ, 341, 41
Smith, E. P., Heckman, T. M., Bothun, G. D., Romanishin, W., & Balick, B. 1986, ApJ, 306, 64
Weedman, D. W. 1973, ApJ, 1973, 183, 29